PROCEEDINGS OF SCIENCE

Remnant Masses and Compact Binary Mergers

Chris L. Fryer[*†]
CCS-2, MS D409, Los Alamos National Laboratory, Los Alamos, NM 87545
E-mail: fryer@lanl.gov

Compact binary mergers are rare events in the universe, but produce many of the brightest observed outbursts observed today. In addition, these mergers play an important role in the production of heavy elements, perhaps dominating the r-process nucleosynthesis as well as iron-peak elements. These mergers are also strong sources of gravitational waves and, if understand fully, can tie gravitational wave measurements to the understanding of matter at extreme conditions. One of the major uncertainties in our understanding of compact remnant mergers is the mass distribution. The mass distribution can help determine the relative rates of different compact binary mergers. Here I review our current understanding of the formation processes behind compact systems, focusing on the mass distribution of these objects.

Frontier Research in Astrophysics,
26-31 May 2014
Mondello (Palermo), Italy

[*]Speaker.

[†]Discussions with Chris Belczynski and Vicky Kalogera led to many projects which formed the basis of this review. This work was carried out in part under the auspices of the National Nuclear Security Administration of the U.S. Department of Energy at Los Alamos National Laboratory and supported by Contract No. DE-AC52-06NA25396.

PoS(FRAPWS2014)004

1. INTRODUCTION

Scientists have invoked a broad range of compact binary mergers and collisions to explain a wide set of astrophysical phenomena. These mergers have been used to explain a wide variety of transients from thermonuclear supernovae to short-duration gamma-ray bursts. Mergers may also dominate the production of heavy elements from silicon and iron peak to r-process elements. They are also proposed sites for gravitational wave (GW) and high-energy neutrino production. Scientists have studied the full range of compact mergers: white-dwarf/white-dwarf (binary white dwarf - BWD), neutron-star/white-dwarf (NSWD) or black-hole/white-dwarf (BHWD) mergers, neutron-star/neutron-star (binary neutron star - BNS), neutron-star/black-hole (NSBH) and binary black hole (BBH) mergers.

Let's review these mergers and their potential role in astrophysics in more detail.

- **BWD:** These mergers (known as the double degenerate scenario in the type Ia supernova community) have been invoked to explain thermonuclear supernovae and almost certainly explain a fraction of the observed distribution of these supernovae: for a review, see [41]. In these mergers, the lower-mass white dwarf is tidally disrupted and the debris accretes onto the more massive white dwarf. Ignition can happen promptly (this is especially the case of collisions) or it can be delayed as the material accretes. The BWD scenario has long been a favorite of scientists modeling binary populations because the predicted rate may be high enough to explain the supernova rate; the single degenerate rate falls well below the observed supernova rate [49]. But the exact emission from these mergers remains a matter of debate [29, 47]. Thermonuclear supernovae play an important role in producing silicon- and iron-peak elements and if BWD dominate the supernova rate, they also are important production sites of these elements. BWD mergers are also an important source for the LISA GW detector [2]. Although most of these mergers are probably produced in binary systems where GW emission drives the BWD interaction, it is possible that triple systems can produce WD collisions and these WD collisions might make up a non-negligible fraction of BWD mergers [40].

- **NSWD/BHWD:** The merger of a white dwarf with either a neutron star or a black hole was originally proposed as a possible progenitor of long-duration gamma-ray bursts [21]. The white dwarf is tidally disrupted well beyond the surface of the neutron star or event horizon of the black hole (unless the black hole is very massive). This tidal disruption forms a very extended disk with a long accretion time > 100 s and it is this black hole (or neutron star) accretion disk that could produce a gamma-ray burst. But these disks can also have explosive burning episodes that might produce a different form of astrophysical transient with yields in the silicon and iron peak elements [42]. However, such mergers are much rarer than BWD mergers (0.0001-15 Myr^{-1} in a Milky-Way massed galaxy: [22, 37]) and are hence not likely to contribute significantly to galactic chemical evolution. The GW signal from these mergers is not in the LIGO passband and these events are too rare to be significant LISA detections.

- **BNS and NS/BH:** The merger of binary neutron star or NS/BH systems are the currently-favored progenitor of short-duration gamma-ray bursts. During the merger, the lower-massed

Merger type	Galactic Merger Rate (Myr^{-1} per MW Galaxy)	Phenomenon
BWD	peak$\sim$ 2000	Type Ia Supernovae, LISA GW source
NSWD,BHWD	0.0001-15	LGRBs, peculiar Supernovae
BNS	0.01-100	SGRBs, aLIGO GW source
NSBH	0.001-50	SGRBs, aLIGO GW source
BBH	0.05-100	aLIGO GW source

Table 1: Properties of Binary Mergers

compact remnant is disruputed, forming a disk around the central core and ejecting a small amount of neutron rich material. In NS/BH and many BNS mergers, the central core is a black hole, and its dense disk of shredded neutron star material produces ideal black hole accretion disk conditions considered the standard mechanism for gamma-ray bursts. The rate (0.01-100 Myr^{-1} in a Milky-Way massed galaxy: [22, 16]) and spatial distribution with respect to their host galaxy [20] of these mergers fits the observations of the short-duration gamma-ray bursts. In some cases, depending upon the equation of state, the central compact object is not sufficiently massive to produce a black hole, and neutron star accretion disks and magnetar accretion disk scenarios[1] are being studied as possible progenitors for gamma-ray bursts with specific, late-time activity. In addition, the neutron-rich ejecta from these mergers may be able to produce most of the r-process elements in universe [39]. Along with BBH, BNS and NS/BH mergers are the primary source of GWs for the advanced LIGO detector [1, 16].

- **BBH:** Although there are some claims the BBH mergers with residual magnetic fields can produce electromagnetic transients, BBH mergers are studied primarily because they could dominate the total rate of sources for advanced LIGO. Current calculations predict that 99% of all LIGO detections could be BBHs [17]. If large black holes masses can be made, these mergers can be detected out to a redshift of 0.5 [5].

Table 1 summarizes the different merger events and the astrophysical phenomena they might produce[2].

Understanding the formation of these objects is important to both determine the relative rates of compact objects and to determine the fate of these mergers. For example, because the masses of black holes can become quite large, the gravitational wave signal from these black holes can drastically alter the detectability of BBHs by advanced LIGO [5]. Accurate mass distribution of black holes is important in determining the viability of these mergers as a LIGO source. Similarly, relative formation rate of NSs and BHs makes a huge difference between the relative rates of BNS, NS/BH, and BBH binaries. Advanced LIGO may be able to estimate these relative rates, provide

[1] As pointed out by the referee, it might be more likely that these mergers produce normal NS magnetic fields. Indeed, with these accretion rates, any magnetic field shoulb be buried.

[2] These rates are primarily based on the latest results (both solar and 0.1 solar metallicity) from the broad studies by [37, 49, 16, 22]. The star formation rate is set to a standard Milky-Way massed galaxy. In the table LGRB, SGRB refer to Long and Short-duration GRBs

direct validation of the core-collapse models. Finally, the neutron star mass distribution determines whether most BNS mergers collapse immediately to black holes, collapse to black holes after some accretion phase, or remain neutron stars. These relative fractions have strong implications for both the gamma-ray burst engine for short-duration bursts as well as advance LIGO gravitational wave sources. Here we will review the formation process and its current predictions on the production and mass distribution of neutron stars and black holes.

2. Supernovae and Compact Remnant Formation

Neutron stars and black holes are formed in the collapse of massive stars. Massive stars go through a series of burning phases, fusing the ashes of previous burning phases until a core of iron is built up in its center. Even after the iron core is formed, shell burning adds to the core mass. The core of a massive star is supported both by thermal pressure and electron degeneracy pressure. As the core gains mass, its weight causes it to compress. With massive enough cores, the compression causes electrons in the core to capture onto protons, each forming a neutron and a neutrino and removing degeneracy pressure. In addition, iron atoms in the core dissociate, removing thermal energy. As these processes remove pressure in the core, the compression accelerates. Within hundreds of milliseconds, the stellar core collapses at nearly free-fall velocities, marking the end of the life of the star and the initiatiation of the supernova explosion.

The core collapses until it reaches nuclear densities, where nuclear forces and neutron degeneracy pressure are able to halt the infall, forming a proto-neutron star. The collapse of stellar cores releases up to 10^{53} erg of gravitational potential energy, a fraction of which is used to power core-collapse supernovae. Although this basic picture has been understood for 3/4 of a century [54, 45, 13], how this energy is converted into explosion energy is still an active area of research.

A number of conversion mechanisms have been proposed to extract this potential energy and understanding these mechanisms allow scientists to place constraints on the compact remnant masses. A number of mechanisms exist invoking magnetic fields that extract rotational energy to drive strong explosions [46, 7, 51]. Magnetic fields are behind the standard models for gamma-ray bursts and their associated hypernovae [52, 48]. However, the convective engine remains the favored model for normal core-collapse supernovae [34]. If correct, this engine will dictate the mass distribution of neutron stars. Indeed, understanding its failure will guide our understanding of the black hole mass distribution as well. In this section, we will study the compact remnant mass distribution under the convective core-collapse supernova engine.

2.1 The Convective Supernova Engine

At the formation of the proto-neutron star, most of the gravitational potential energy has been converted into thermal energy in the core, mostly in the form of neutrinos (even neutrinos are trapped at these nuclear densities). The core bounces, driving a shock through the star. The bounce shock progresses up into the imploding star. To drive an explosion, the shock must reverse this infalling material, accelerating it to a high enough velocity to escape the cores gravitational potential well. However most of the energy in the shock is in neutrinos, and when the shock becomes diffuse

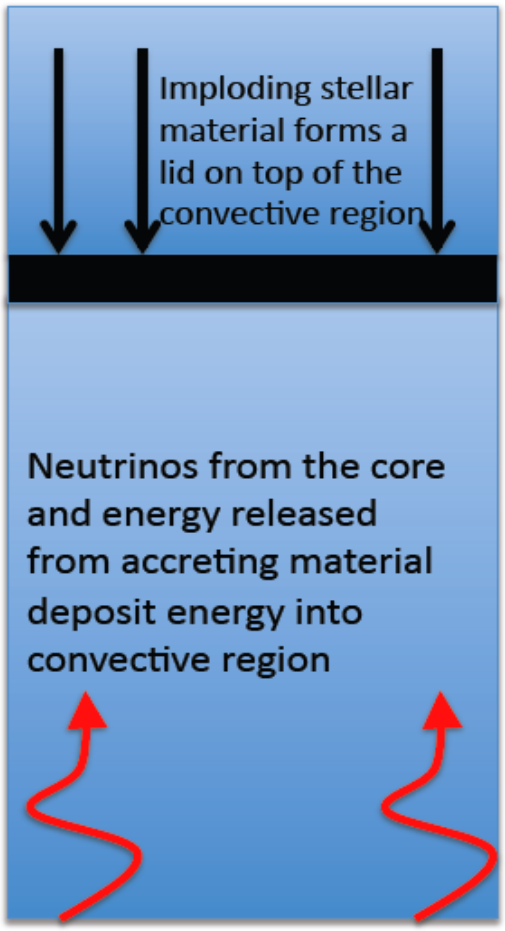

Figure 1: Diagram of the 1-dimensional picture of core-collapse supernovae. At the bottom of the diagram is the hot proto-neutron star, leaking neutrinos. At the top is the infalling star, piling up where the initial bounce shock stalled. This proto-neutron star is a heating source and the infalling material is a lid of this supernova-engine pressure cooker. In 1-dimension, the energy deposited at the base must diffuse/advect through this bounded region until there is enough energy in this region to blow off the lid.

enough for the neutrinos to leak out, its energy is lost and it stalls. Reviving the stalled shock has been the focus of supernova modelers for the past 5 decades.

To understand the formation of neutron stars and black holes, we must understand this post-bounce scenario. Figure 1 shows a 1-dimensional picture of the stellar core after the stall of the shock. Between the proto-neutron star surface and the stalled shock is a region that is heated below by neutrino emission and bounded at the top by the stalled shock. As the rest of the star falls onto the stalled shock, it forms a lid to this neutrino-driven pressure cooker. If sufficient energy can be deposited into this bounded region so that it can blow of this lid, a supernova is produced.

Whether or not an explosion is produced depends upon both the efficiency of the heating and the strength of the lid. In 1-dimension, as stellar material piles up on the stalled shock, the pressure required to blow off the lid and drive an explosion increases with time. The neutrino emission arises

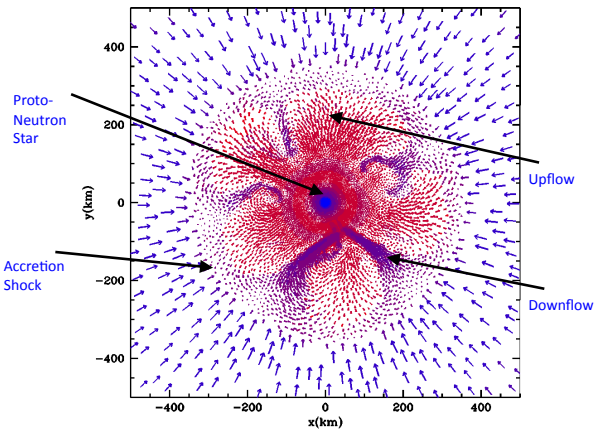

Figure 2: Slice of a 3-dimensional simulation of the core-collapse engine. The direction and length of the vectors denote the magnitude and direction of the velocity. The coloring corresponds to the entropy (light colors are high entropy, dark colors are low entropy). Low entropy material falling onto the stalled shock flows down toward the proto-neutron star surface. Energy deposition (either in the form of internal or turbulent energy) near the proto-neutron star surface causes material to rise. The primary differences with the 1-dimensional picture is that the material does not pile up at the shock, but flows down to the core. This leads to a weaker "lid", provides more energy at the base at the top of the proto-neutron star and converts the energy deposited more quickly to kinetic energy. For more details, see [25, 28].

solely from the proto-neutron star, heating a region just above the proto-neutron star surface. But in 1-dimension, the energy just above the surface must diffuse its energy to the rest of the bounded region. With the ever-increasing lid strength and the slow diffusion time to transport energy, driving an explosion is difficult. Except for very low-mass stars where the infalling material is so low-mass that it is easy to explode (e.g. ONe cores [23, 38]), 1-dimensional simulations fail to achieve explosions.

It has long been known that multi-dimensional effects could enhance the energy deposition above the shock. Convection in the proto-neutron star was invoked to accelerate the transport of the neutrinos out of the core, increasing the deposition rate of energy in the bounded region [18]. But the bounded region is also convectively unstable, and it is this convective region that has been the focus of most supernova engine studies for the past 2 decades [34, 12, 36, 9, for example]. Figure 2 shows a 2-dimensional slice of one of the early 3-dimensional models of the stellar collapse [28]. The vectors in the image denote the magnitude and direction of the material motion while the shading denotes the entropy.

As can be seen in the image, there is a strong entropy gradient in this model. After the bounce of the core, the shock moved through the silicon shell, decelerating as it moved outward until it stalled. This shock left behind a negative entropy-gradient profile ($\partial S/\partial r < 0$). Typical growth times for this entropy-driven, or Rayleigh-Taylor, instability are on the order of ~ 2 ms[28]. As colder material piles up at the stalled shock, it can overcome the pressure of the convective region,

driving downflows. Nutrinos from the hot proto-neutron star continue to heat the region above the proto-neutron star, driving further convection. Additional instabilities can occur, e.g. the vortical acoustic instability first studied by [35] and re-investigated for the supernova engine by [9]. However, this mechanism has a much longer growth time than the entropy-driven convection and unless the entropy-driven convection can be damped, it is likely that Rayleigh-Taylor instabilities dominate the convective motions. [30] studied 2 separate scenarios for compact remnant masses, one assuming a fast-growth instability mimicking Rayleigh-Taylor, the other assuming a slower-growing instability to mimic the slower-growing vortical acoustic instabilities.

Figure 2 provides the basic picture from which we can build our intuition on the supernova engine and compact remnant mass distribution. The convective region above the proto-neutron star will continue to boil until it either overcomes or is crushed by the ram pressure of the stellar material falling onto the stalled shock. By comparing the multi-dimensional and 1-dimensional pictures, we can better understand why convection can play an important role in the explosion:

- **Reducing the strength of the lid:** In the 1-dimensional model, imploding material piles up on the stalled shock that forms the lid to our supernova engine "pressure cooker". In 1-dimension, the amount of energy required to drive an explosion increases as the mass increases and hence the explosion becomes harder to explode with time. In multi-dimensions, the cold material piling up at the shock is convected to the neutron star surface and no material piles up at the shock. This means that it does not get more difficult to explode the supernova with time. Indeed, because the infalling accretion rate decreases with time, it actually gets easier.

- **More efficient use of neutrino energy:** In the 1-dimensional model, material just above the neutron star surface absorbs neutrinos from the core and this heat the diffuses through the convective region. This heat diffusion is inefficient and this process can be too slow to drive an explosion. In multi-dimensions, convection transports this energy throughout the convective region very quickly (recall the 2 ms growth timescale).

- **More energy sources:** In multi-dimensions, we also have additional energy sources. As we discussed, the material does not pile up on the shock, but is convected downwards to the proto-neutron star surface. This releases additional gravitational potential energy that can heat the convective core through additional neutrino heating or pressure waves (e.g. advective-acoustic processes [19]) and turbulent energy [15].

By enhancing both the energy deposition and the conversion to kinetic energy and reducing the strength of the lid, convection above the proto-neutron star has been shown in simulations to produce explosions[25, 26, 11, 10], but we are far from a quantitative explosion model and much more work must be done before understand all the details of this supernova engine. We will term this engine the convection-enhanced engine. This convection-enhanced engine has become the standard model for normal supernovae, in part because it has the ability to explain features in the current supernova observations. As such, we will focus on this model in discussing the supernova engine.

Some supernovae may be produced through strong magnetic fields in rotating collapsing systems and many of these mechanisms predict bipolar explosions [51, 32], although it has been argued

that a pure dipole magnetic structure is required to produce even a weak bimodal explosion [3, 43]. Well-studied supernovae such as Cas A [31] and SN 1987A [8], although arguing for low-mode explosions, do not show evidence for a bipolar jet-like outburst. This argues that most supernovae are not produced through these magnetic mechanisms.

2.2 Explosion Energy

Until the discovery of exotic (and rare) energetic supernovae such as hypernovae (first discovered associated with gamma-ray bursts) and superluminous supernovae, all the observed supernovae seemed to produce explosions energies clustered around one to a few foe[3]. Any core-collapse model invoking the collapse of a massive star must explain how only 1% of the 10^{53} erg of energy released in the collapse of an iron core goes into producing the supernova explosion. The evidence that supernovae are produced in the collapse of massive stars is strong, from a growing list of progenitor observations[50] to the neutrinos detected in SN 1987A[33, 6]. Observations of gamma-ray bursts suggest that some (generally magnetic field) mechanisms can be more efficient at extracting the energy. But for most supernovae, the explosion energy never exceeds roughly a few percent of the gravitational energy released. Any model for these outbursts should have an explanation for why it is only able to extract a few % of the total energy budget. As we shall show here, the convection-enhanced mechanism provides a natural explanation for this low efficiency.

In this engine, the energy of the convective region continues to increase until it has enough energy to blow off the lid. That is, its energy increases until the pressure in the convective region is larger than the pressure produced by the infalling matter. We can estimate the pressure in the convective region by assuming the convection pushes this region toward constant entropy. The pressure profile in the convective region is then given by[30]:

$$\begin{aligned} P(r) &= [0.25 M_{\rm NS} G (S_{\rm rad}/S_0)^{-1} (1/r - 1/r_{\rm shock}) \\ &\quad + P_{\rm shock}^{1/4}]^4 {\rm erg\,cm^{-3}} \end{aligned} \tag{2.1}$$

where $M_{\rm NS}$ is the proto-NS mass, G is the gravitational constant, $S_{\rm rad}$ is the entropy in Boltzmann's constant per nucleon, $S_0 = 1.5 \times 10^{-11} {\rm k_B\,per\,nucleon}$, $r_{\rm shock}$ and $P_{\rm shock}$ are the radius and pressure of the accretion shock forming the outer bound of the convective region. $P_{\rm shock}$ is set to the ram pressure of the infalling material. If we assume that the infalling material does not pile up (because it quickly sinks down toward the proto-neutron star, the convective region is bounded by a lid entirely by the ram pressure of the infalling material descending at the free-fall rate[27]:

$$\begin{aligned} P_{\rm shock}(r) &= 1/2 \rho_{\rm shock} v_{\rm free-fall} \\ &= (2GM_{\rm NS})^{0.5} \dot{M}_{\rm acc} / (8\pi r_{\rm shock}^{2.5}) \end{aligned} \tag{2.2}$$

where the free-fall velocity ($v_{\rm free-fall}$) is determined by the proto-NS mass and the accretion rate $\dot{M}_{\rm acc}$ is determined by the structure of the progenitor star assuming a pressure-less collapse (which the infall nearly is). For a radiation-dominated gas, the internal energy density is $3 \times P(r)$ [27]:

$$u(r) = 3 \left[4.7 \times 10^8 \frac{M_{\rm NS}}{M_\odot} \frac{10 k_{\rm B} {\rm nuc}^{-1}}{S_{\rm rad}} \left(\frac{10^6 {\rm cm}}{r} - \frac{10^6 {\rm cm}}{r_{\rm shock}} \right) + \right.$$

[3] Termed by Hans Bethe, the foe stands for ten to the Fifty One Erg. This unit has, after Hans Bethe's death, also been named the Bethe. I leave it to the reader to determine which Bethe, with his sense of humor, would have preferred.

$$1.2\times10^{6}\left(\frac{M_{\rm NS}}{M_\odot}\frac{\dot{M}_{\rm acc}}{M_\odot {\rm s}^{-1}}\right)^{1/4} \left(\frac{2\times10^{7}{\rm cm}}{r_{\rm shock}}\right)^{5/8}\Bigg]^{4} {\rm erg\,cm^{-3}}. \quad (2.3)$$

If we assume that the free-fall ram pressure is the entire strength of the lid (this is a slight underestimate as some material does pile up and its mass should be included) and we assume that as soon as the convective region starts to move the shock outward, no further energy deposition occurs (this too, will underestimate the energy), for a giving infall rate, we can determine the explosion energy. Figure 3 shows the infall rate for a variety of stellar models with masses range from 12 to $40M_\odot$ as a function of time after bounce. There are a few trends to note in these models: (1) the basic infall rate initially decreases with time (meaning that it will be easier to drive the explosion at later times) and (2) the infall rate increases with increasing progenitor mass (meaning it will be more difficult to drive explosions of more massive stars). Not surpisingly, this latter trend explains why simulations of 1-dimensional explosions are only successful for the lowest-mass progenitors and no models can explode the more massive stars even with the convection-enhanced mechanism. Although these trends exist, the differences between these progenitors are not so great. If the engine was truly robust, all stellar collapses should explode. The fact that core-collapse must produce both normal supernovae and fizzles that produce black holes makes it clear that detailed calculations are required to get quantitative results (explaining the difficulties facing the supernova engine community). It also argues that any explosion mechanism must be just at the edge of success and failure (it is possible to argue under the rotating/magnetic field model that the variation in the spin rate causes the range of results).

Using these infall accretion rates and setting the explosion energy to the energy stored in the convective region, we can then estimate the explosion energies as a function of how long it takes the explosion to occur (Fig. 4). If the explosion can happen quickly, a 1-2 foe explosion is produced, but if it takes 500 ms for the convective engine to work, it is difficult to produce explosions that are stronger than a few tenths of a foe. When the explosion occurs depends upon how quickly energy can be deposited in the convective region. This depends on both how rapidly the energy from the core can reach the proto-neutron star surface (hence, the convection within the proto-neutron star is still important), but also on how quickly the convection in the region above the neutron star can develop into full-blown convection. For example, in our case of Rayleigh-Taylor instabilities with their growth time of 2 ms, strong turbulence develops quickly and and for many models, an explosion will occur in the first 150-200 ms. In contrast, the much slower growing vortical-acoustic instability ($\sim 75-100$ times slower growth times), it is unlikely that th explosion will occur until 500 ms after bounce.

Figure 4 also includes the energy growth for these two different models, where the rapid model stars with a very low energy, but with a doubling time of 10 ms. The delayed explosion is initiated with twice the amplitude, but a doubling time of 200 ms. Where this energy exceeds the energy required to blow off the lid, an explosion occurs. Although such estimates are rough, in general, the rapid explosions mimicking Rayleigh-Taylor produce much more energetic explosions than those instabilities requiring longer growth times. In either case, the explosions are peaking near the 1-2 foe energies required by observations.

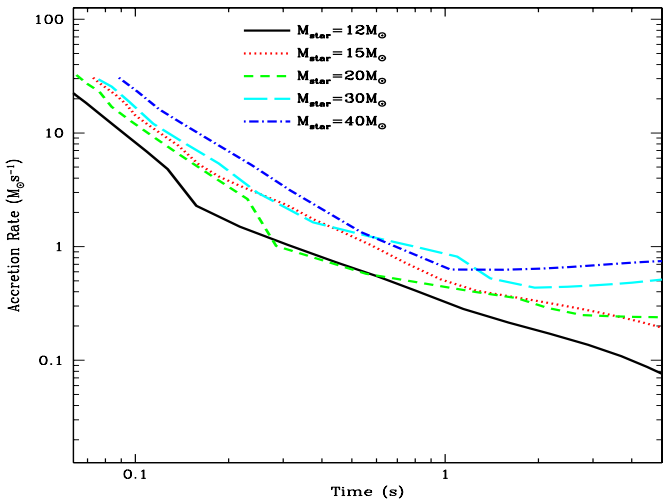

Figure 3: Accretion rate versus time for 5 different stellar models produced using the Kepler code [53]. There is a general trend where the accretion rate increases with initial zero-age main sequence mass, arguing that it is more difficult to explode more massive stars. However, it also argues that if these stars do explode, their explosion energies could be more energetic than lower mass stars. Unfortunately, a number of uncertainties remain in modeling massive stars, including the simplified models for the late stages of thermonuclear burning[4] and it is difficult to make firm predictions. However, if the trend continues that, in general, larger stars make larger cores, it is likely that larger stars will be harder to explode.

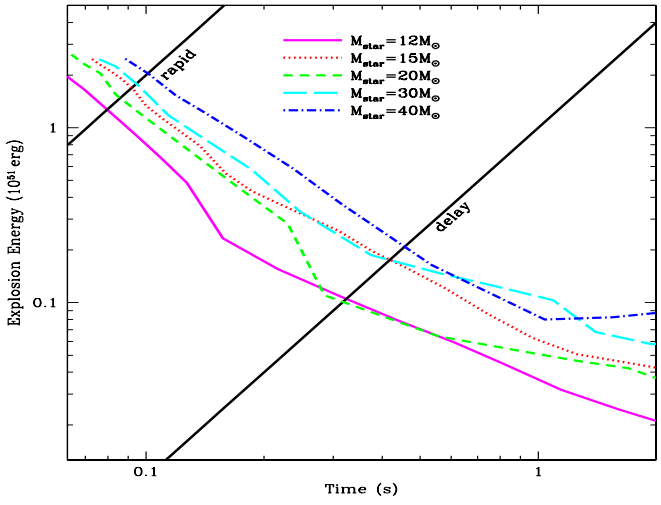

Figure 4: Explosion energies as a function of time for the 5 models in figure 3. Depending upon the growth rate of the convection, the explosion can occur quickly or $>$ 300 ms after bounce. This growth time dictates the explosion energy.

Recall that we made several assumptions in these derivations. First, we assumed that no mass piles up at the stalled shock. If there is even a small amount of pile up (a fraction of a solar mass), the required explosion energy can double. In addition, we have assumed that energy deposition stops when the explosion occurs. In a symmetric explosion, this is reasonable. As the density decreases, neutrinos no longer deposit their energy, turning off the heating. But in a turbulent engine, material continues to accrete onto the neutron star after the shock is expanding, allowing a longer driving phase. Both of these could easily allow explosions that are a factor of a few above the results here. Nevertheless, the energies remain in the 0.5-5 foe range, naturally fitting the observed energies of normal supernovae[4].

Let's review the observational constraints fit by these models:

- **Core collapse produce both neutron stars and black holes - explosions and fizzles:** Although progenitors have only mild differences[5], the convection-enhanced mechanism can produce both strong supernova explosions and fizzles or failed explosions.
- **Most Supernovae have explosion energies of a few foe, a few percent of the potential energy released in the collapse of the core:** Because the energy is limited to the energy stored in the convective region, this low efficiency is naturally explained by the convective engine model.
- **Low-mode Explosions in Remnants:** Low-mode convection in the supernova engine predicted the low-mode (but not bipolar) ejecta seen in remnants.

2.3 Compact Remnant Masses

With an estimate for the explosion energy, we can now calculate the remnant mass. One simple approach is to assume that the explosion energy (or a constant fraction thereof) goes into unbinding the star. We can calculate the binding energy at every mass coordinate - that is, the binding energy of all the material beyond a given mass coordinate ($\int_M^\infty BE dM$ where M is the mass coordinate and BE is the binding energy). Determining where the explosion energy equals the binding energy provides a rough estimate for the final remnant mass. Figure 5 shows the binding energy for a range of stellar models. The energy required to eject all but the inner $1.5\,M_\odot$ of a $12\,M_\odot$ is only a few tenths of a foe. For a $30\,M_\odot$ star, a 1 foe explosion would still leave behind a $5\,M_\odot$ black hole. The large variation in binding energy between stars is why even rough calculations of the explosion energy can make reasonably accurate estimates of the compact remnant mass.

[24] used this strong dependence to argue that somewhere between 18-23$M_\odot$ is the demarcation dividing systems that make black holes versus systems that make neutron stars[6]. There are quite a few caveats with this estimate. For example, mass loss for the most massive stars can considerably alter both the core and the binding energy such that a star with an initial zero-age main

[4]Note that the analysis of the explosion energy in normal supernovae also has its pitfalls and its errors may also lie in the factor of a few range.

[5]Indeed, [30] has shown that the differences between the results of two different stellar evolution codes are often bigger than the differences caused by mass or metallicity.

[6]This assumes mass loss from stellar winds is a minor effect. If mass loss can alter the core (in some models, a $40\,M_\odot$ star ends its life with less than $3\,M_\odot$, a likely progenitor for a neutron star), the fate becomes les monotonic with progenitor mass.

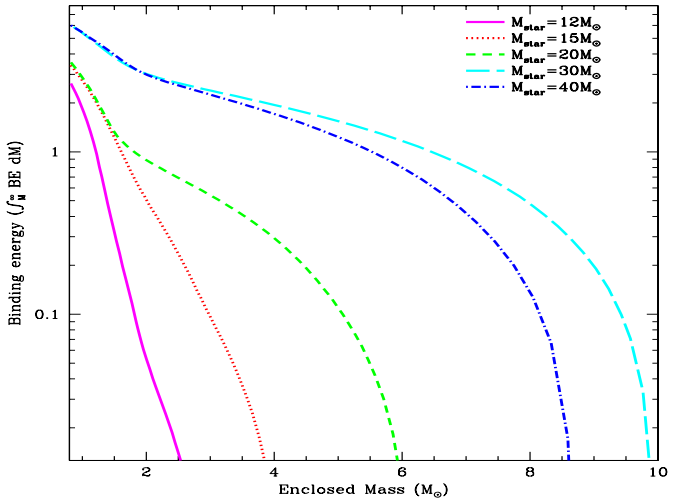

Figure 5: Binding energy of all stellar material outside of a given enclosed mass and a range of initial progenitor masses. This plot shows the amount of energy needed to eject the star for a given remnant mass set to the enclosed mass. In some sense, this is an overestimate in the energy since the star has internal energy on par with the binding energy (although the star is initially at equilibrium, it loses considerable energy in the collapse due to neutrino emission). In practice, since the matter is ejected with twice its escape velocity, this estimate provides a good rule of thumb for the explosion energy. With all these caveats, note that, for a low initial stellar mass, the binding energy is minimal. If the collapse leaves behind a remnant with a baryonic mass of $2\,M_\odot$ (roughly a $1.8\,M_\odot$ gravitational mass), the energy needed for a low mass progenitor is only a few % of a foe. For a $40\,M_\odot$ star, the explosion energy must exceed a few foe. If such a massive star explodes, it is likely to have considerable fallback, ultimately producing a black hole.

sequence mass much higher than another star can end its life with a much smaller core. In addition, mixing in stars remains an active area of research and small modifications in mixing algorithms can drastically alter the core mass and hence its binding energy.

The binding energy in figure 5 neglects any thermal support. Technically, this thermal energy nearly balances the gravitational potential energy. The binding energy estimate really assumes that the material is ejected at roughly its escape velocity, requiring material deeper within the gravitational well to have stronger energies. This assumption sweeps under the rug much of the physics needed to model this ejecta. However, it does match more detailed simulations fairly well.

Under these assumptions, one can calculate the remnant mass as a function of the progenitor. Figure 6 plots the remnant mass assuming rapid explosions for a range of initial stellar masses and metallicities. The dashed/dotted lines show the results applied to specific models and the solid lines are fits to those models. Note that because the evolution of the stellar models is not linear with mass, there is quite a bit of structure in the function comparing the remnant mass to the initial zero-age main sequence star mass. The equivalent figure for a delayed model is shown in figure 7. The change in the remnant mass distribution is more gradual with this model.

As we have shown, using core-collapse calculations as a guide, we can estimate the mass distribution of compact remnants. However, this required a series of calculations:

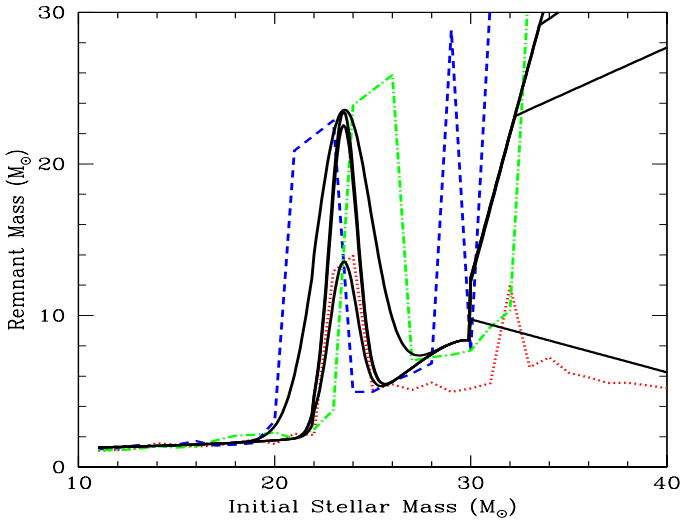

Figure 6: Remnant masses as a function of initial progenitor mass (dotted - solar, dashed - 10^{-4} solar, dot-dashed - zero metallicities). The solid curves are fits assuming a rapid explosion from a remnant model to this data. This figure is from [30], reprinted with permission. The peak in remnant masses around $\sim 23\,M_\odot$ corresponds to an instability in the mixing. Research is now trying to determine whether such instabilities are physical or numerical artifacts of the 1-dimensional stellar evolution codes.

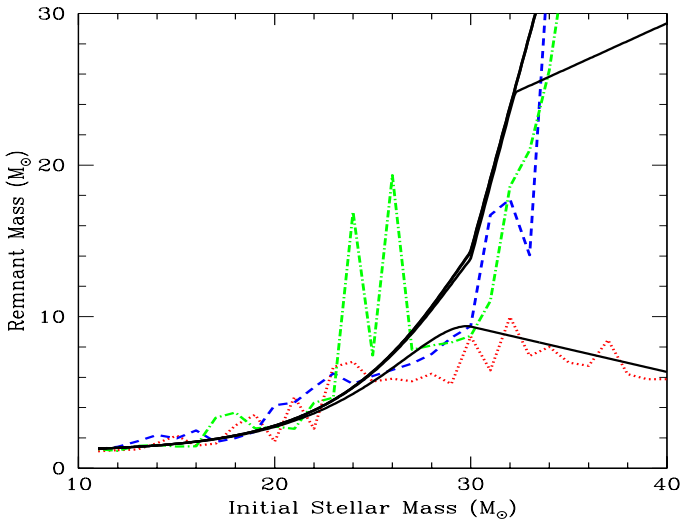

Figure 7: Remnant masses as a function of initial progenitor mass (dotted - solar, dashed - 10^{-4} solar, dot-dashed - zero metallicities). The solid curves are fits assuming a delayed explosion from a remnant model to this data. In comparing this figure to figure 6, contrast the gradual increase in mass with progenitor mass in the delayed case against the virtually constant mass followed by a steep increase in mass with progenitor mass in the rapid-explosion case. This means the delayed explosions produces a broader range of compact remnant masses (all the way through the reportedly obserced mass gap between 2 and $4\,M_\odot$. This figure is from [30], reprinted with permission.

- **Estimate Infall Rate:** Using the stellar structure, we must estimate the infall rate as a function of time. Here we assume the star contracts at free-fall velocities.
- **Estimate Energy Deposition:** Assuming that the convection occuring between the proto-neutron star and the stalled shock is the bottleneck in depositing energy, we can estimate a growth time for the energy in this convective region. Comparing this energy to the energy required to blow off the lid produced by the ram pressure of the infalling material, we can get an explosion energy.
- **Binding Energy:** Calculate the gravitational binding energy of the star and compare this binding energy to the explosion energy to estimate the final compact remnant mass.

2.4 Comparison to Compactness

For many stellar modelers, just a rough idea of the final fate of the massive star is sufficient. To estimate that, [44] developed an estimate that covers the basic structure of the star which they called the compactness parameter (ξ):

$$\xi_{\mathrm{M_{crit}}} = \frac{M_{\rm crit}}{M_\odot} \frac{1000\,km}{R(M = M_{\rm crit})} \tag{2.4}$$

where $M_{\rm crit}$ is a critical mass, typically chosen to be around $2.5\,\mathrm{M}_\odot$ and $R(M = M_{\rm crit})$ is the radial coordinate of this critical mass after bounce. It turns out that the answer is not too different (and all trends remain identical) if one calculates the compactness parameter at collapse, allowing stellar modelers to quickly estimate the fate of their stars.

Figure 8 shows the values for ξ for our suite of models using a range of values for $M_{\rm crit}$. The choice of $M_{\rm crit}$ changes the value for ξ but the trend in this quantity is robust over a wide set of values for $M_{\rm crit}$. For a choice of $M_{\rm crit}$, there is a value for ξ above which the star will not produce a supernova explosion and, instead, collapse to form a black hole. This has been studied in detail using 1-dimensional models by [44].

Prior to this "compactness parameter", most scientists used the entropy of the core to get a rough estimate of the fate of the star. Are these quantities equivalent? Let's try and understand this quantity in a bit more detail. For a constant entropy atmosphere in equilibrium, the density profile (and mass profile) of the atmosphere can be derived as a function of the entropy. If we assume a radiation dominated gas, the mass is given by [14]:

$$M = 4\pi(1/4M_{\rm ns}G)^3(S_{\rm rad}/S_0)^{-4} ln(R/R_{\rm ns})\, g \tag{2.5}$$

where $M_{\rm ns}, R_{\rm ns}$ are the mass and radius of the proto-neutron star after the bounce of the core, G is the gravitational constant, and $S_0 = 1.4 \times 10^{11}$. Solving for entropy, we find:

$$(S_{\rm rad}/S_0)^4 = \frac{M}{(1/4M_{\rm ns}G)^3 ln(R/R_{\rm ns})}. \tag{2.6}$$

In such a case, there is a one-to-one correspondence between entropy and compactness parameter and, just like with ξ, there is a value for the entropy, below (instead of above) which

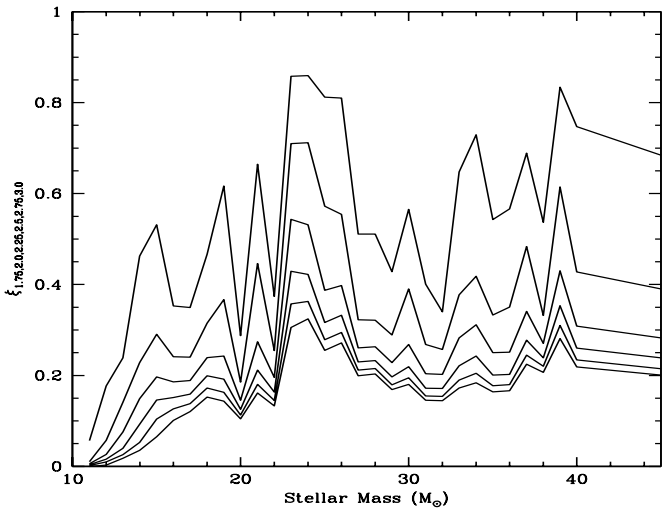

Figure 8: Compactness parameter for the set of solar-metallicity progenitors we used for our remnant mass plots using a range of critical compactness-parameter masses, M_{crit}: 1.5,1.75,2.0,2.25,2.5,2.75. The trends hold regardless of the choice of the critical mass within this range. Not surprisingly, the compactness parameter increases with increasing progenitor mass, echoing our more detailed models. Not also the peak near a zero-age main-sequence mass of 24 $M_\odot$ that matches our remnant mass.

the star will not produce a supernova explosion. Of course, this derivation made several assumptions (radiation pressure dominating the pressure, constant entropy) and the picture gets a bit muddier when one tries to look at actual stars, but the trends between entropy and the fate of the star will persist.

Whether one uses entropy or compactness parameter, we still face the problem of using these simple quantities to determine the fate of the core. How do these simplified quantities compare to our more detailed analysis? In figure 9, we compare remnant masses for our rapid and delayed explosions against the value for ξ for their progenitor models. Although the basic trends agree, there is some scatter, especially at the transition between black hole and neutron star formation.

Compactness is an easily calculable quantity to determine the fate of a massive star and it provides the basic trends in the fate of these stars. It is essentially equivalent to the inverse of the entropy and either could be used to get a first guess to the fate of the star. However, to better understand the fate of the star and, in particular, the mass of the remnant, more detailed calculations are required. Our discussion in section 2.3 provides a more direct relation to the pertinent physics and this methodology is required to do a 2nd order improvement on the simple compactness or entropy parameters.

3. Conclusions

Compact binary megers have been invoked to explain a wide variety of astrophysical tran-

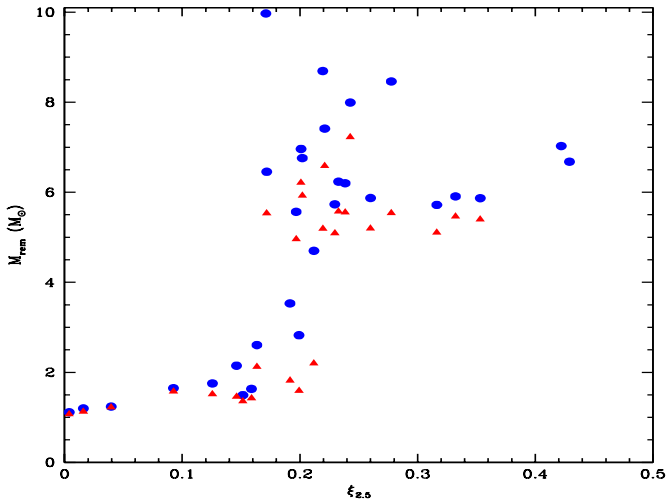

Figure 9: Remnant mass using our more detailed analysis (both rapid and delayed explosions) versus compactness parameter. There is a basic trend between compacntess parameter ($M_{crit} = 2.5$) and remnant mass although, especially at the boundary, here roughly at a compactness parameter of 0.2, it is difficult to gauge the mass from the compactness parameter. Clearly the compactness parameter or entropy of a star does give a first guess toward the fate of a star, but more detailed analyses are needed to determine its fate.

sients including the most energetic explosions in the universe: supernovae and gamma-ray bursts. Whether or not the compact remnant is a black hole or a neutron star can drastically change the obserational consequences of the merger. Further, even the mass distributions of the compact remnants can alter the fate of their mergers. For example, the merger of two 1.1 $M_\odot$ neutron stars is likely to form a neutron star (or magnetar) system. Although this merger will no doubt form an interesting transient, it may not produce the high Lorentz-factor jets seen in short-duration gamma-ray bursts. Such a system could have a very different than the merger of two 2.0 $M_\odot$ neutron stars that form a black hole accretion disk, the standard mechanism for gamma-ray bursts.

Here we have reviewed the physics behind supernovae and compact remnant formation, focusing on the mass distribution of compact remnants. Under the convective engine paradigm, the progenitor structure and the time of explosion dictates the final remnant mass. Both entropy or compactness parameters can be used to obtain both an estimate of the fate of the star and the distribution of progenitor masses. With slightly more careful analysis, remnant masses can be estimated based on the growth time of the convection. In this manner, remnant masses provide a means to study the supernova engine itself.

References

[1] Abadie, J., Abbott, B.P., Abbot, R., et al. 2010, CQGra, 27, 173001

[2] Amaro-Seoane, P., et al. 2013, GW Notes, Vol. 6, p. 4-110 6:4-110

[3] Ardeljan, N.V., Bisnovatyi-Kogan, G.S., Moiseenko, S.G. 2005, MNRAS, 359, 333

[4] Arnett, W.D., Meakin, C. 2011, ApJ, 733, 78

[5] Belczynski, K., Buonanno, A., Cantiello, M., Fryer, C.L., Holz, D.E., Mandel, I., Miller, M.C., Walczak, M. 2014, ApJ, 789, 120

[6] Bionta, R.M., Blewitt, G., Bratton, C.B., Casper, D., Ciocio, A. 1987, PhRvL, 58, 1494

[7] Bisnovatyi-Kogan, G.S. 1971, Soviet Astron.-AJ, 14, 652

[8] Boggs, S., et al. 2015, submitted to Science

[9] Blondin, J.M. Mezzacappa, A. DeMarino, C. 2003, ApJ, 584, 971

[10] Bruenn, S.W., et al., astro-ph/1409.5779

[11] Buras, R., Rampp, M., Janka, H.-Th., Kifonidis, K. 2006, A&A, 447, 1049

[12] Burrows, A., Hayes, J., Fryxell, B.A. 1995, ApJ, 450, 830

[13] Colgate, S.A., & White, R.H. 1966, ApJ, 143, 626

[14] Colgate, S.A., Herant, M., Benz, W. 1993, Phys. Rep., 227, 157

[15] Couch, S.M., Ott, C.D. 2014, astro-ph/1408.1399

[16] Dominik, M., Belczynski, K., Fryer, C., Holz, D.E., Berti, E., Bulik, T., Mandel, I., O'Shaugnessy, R. 2012, ApJ, 759, 52

[17] Dominik, M., Berti, E., O'Shaugnessy, R., Mandel, I., Belczynski, K., Fryer, C., Holz, D.E., Bulik, T., Pannarale, F. 2014, submitted to ApJ, astro-ph/1405.7016

[18] Epstein, R.I. 1979, MNRAS, 188, 305

[19] Foglizzo, T., Galleti, P., Scheck, L., Janka, H.-Th. 2007, ApJ, 654, 1066

[20] Fong, W., Berger, E. 2013, ApJ, 776, 18

[21] Fryer, C.L., Woosley, S.E., Herant, M., & Davies, M.B. 1999, ApJ, 516, 892

[22] Fryer, C.L., Woosley, S.E., Hartmann, D.H. 1999, ApJ, 526, 152

[23] Fryer, C.L., Benz, W., Herant, M., Colgate, S.A. 1999, ApJ, 516, 892

[24] Fryer, C.L. 1999, ApJ, 522, 413

[25] Fryer, C.L., & Warren, M.S. 2002, ApJ, 574, L65

[26] Fryer, C.L., & Warren, M.S. 2002, ApJ, 601, 391

[27] Fryer, C.L. 2006, New Astronomy, 50, 492

[28] Fryer, C.L., & Young, P.A. 2007, ApJ, 659, 1438

[29] Fryer, C.L., et al. 2010, ApJ, 725, 296

[30] Fryer, C.L., Belczynski, K., Wiktorowicz, G., Dominik, M., Kalogera, V., Holz, D.E. 2012, ApJ, 749, 91

[31] Grefenstette, B.W., et al. 2014, Nature, 506, 339

[32] Hayato, M., Sato, Y., Matsumoto, T., Hanawa, T. ApJ, 683, 357

[33] Hirata, K., Kajita, T., Koshiba, M., Nakahata, M., Oyama, Y. 1987, PhRvL, 58, 1490

[34] Herant, M., Benz, W., Hix, W.R., Fryer, C.L., Colgate, S.A. 1994, ApJ, 435, 339

[35] Houck, J.C., & Chevalier, R.A. 1992, ApJ, 395, 592

[36] Janka, H.-T. & Müller, E. 1996, A&A, 306, 167

[37] Kalogera, V., Kim, C. Lorimer, D.R., Ihm, M., Belczynski, K. 2005, in Binary Radio Pulsars, ASP Confernce Series, Vol. 328, ed. F.A. Rasio and I.H. Stairs

[38] Kitaura, F.S., Janka, H.-Th., Hillebrand, W. 2006, A&A, 450, 345

[39] Korobkin, O., Rosswog, S., Arcones, A., Winteler, C. 2012, ApJ, 426, 1940

[40] Kushnir, D., Katz, B., Dong, S., Livne, E., Fernández, R. 2013, ApJ, 778, L37

[41] Maoz, D., Mannucci, F., Nelemans, G. 2014, ARA&A, 52, 107

[42] Metzger, B.D. 2012, MNRAS, 419, 827

[43] Moiseenko, S.G., Bisnovatyi-Kogan, G.S., Ardeljan, N.V. 2006, MNRAS, 370, 501

[44] O'Connor, E., Ott, C.D. 2011, ApJ, 730, 70

[45] Oppenheimer, J.R., Volkoff, G.M. 1939, Phys. Rev. 55, 374

[46] Ostriker, J.P. & Gunn, J.E. 1971, ApJ, 164, L95

[47] Pakmor, R., Kromer, M., Taubenberger, S., Sim, S.A., Röpke, F.K., Hillebrandt, W. 2012, ApJ, 747, L10

[48] Popham, R. Woosley, S.E., Fryer, C. 1999, ApJ, 518, 356

[49] Ruiter, A.J. Belczynski, K., Fryer, C. 2009, ApJ, 699, 2026

[50] Smartt, S.J. 2009, ARA&A, 47, 63

[51] Wheeler, J.C. Meier, D.L., Wilson, J.R. 2002, ApJ, 568, 807

[52] Woosley, S.E. 1993, ApJ, 405, 273

[53] Woosley, S.E., Heger, A., Weaver, T.A. 2002, Rev. Mod. Phys., 74, 1015

[54] Zwicky, F. 1938, ApJ, 88, 522